The shell structure of π ring currents in the expanded porphyrin amethyrin

Erich Steiner[a] and Patrick W. Fowler*[b]

Received 17th February 2006, Accepted 28th April 2006
First published as an Advance Article on the web 18th May 2006
DOI: 10.1039/b602426b

Direct *ab initio* mapping of induced current density in the π system of the expanded porphyrin amethyrin shows a picture at variance with the conventional $4n$ π ascription of antiaromaticity. The ipsocentric orbital model interprets the pattern of currents as a superposition of shell contributions: an intense paratropic ring current concentrated on the inner 20-site cycle, counteracted by a weaker diatropic circulation on a 24-site conjugation pathway and a combination of local 5-site diatropic circulations on the six pyrrolic rings.

1. Introduction

Porphyrins and their synthetic analogues,[1–3] the expanded, contracted and isomeric porphyrins, present the theoretician with a considerable challenge for the interpretation of their magnetic properties. Recent theoretical work on these "decorated macrocycles" has suggested that the pyrrolic groups, which make up the decorations, present only a small barrier to the global ring current around the macrocycle in the presence of a perpendicular magnetic field.[4–6] In addition, it has been shown that the global ring currents, at least in the systems presented so far, follow closely the 4- and 2-electron rules which, in the ipsocentric formulation of magnetic properties, are the analogues of the $(4n + 2)$ and $(4n)$ Hückel rules for aromaticity and antiaromaticity of annulenes. In the present work, however, direct *ab initio* mapping of induced current density in the π system of the expanded porphyrin amethyrin (**1**) shows a picture at variance with this simple scheme.

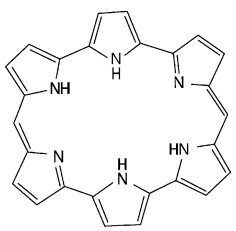

1

Amethyrin was first reported in 1995 by Sessler and co-workers[1] as one of two expanded porphyrins, with orangarin, whose cyclic π conjugation pathways fit Hückel's $4n$ rule for antiaromaticity in annulenes (24 π electrons in amethyrin, 20 in orangarin, making the conventional choice). ^{1}H NMR spectra of both molecules show large downfield shifts for the internal NH protons and upfield shift for the bridge CH protons, and these shifts are consistent with the presence of a global paratropic ring current. Some doubt remained, however, as to the origin of the chemical shifts.[1,2]

In a recent comparative study of sapphyrin and orangarin,[5] we showed that, within the ipsocentric orbital model of current density,[7–10] the global diatropic π ring current in sapphyrin and the global paratropic ring current in orangarin are predominantly properties of the frontier orbitals, with HOMO–LUMO transitions making by far the largest contributions to the current density. Thus, in common with other physical and chemical properties that distinguish the whole molecule from its parts, the global response of a molecule to an external magnetic field is largely a property of its most mobile electrons: those with the most ready access to excited states. Specifically, for annulenes,[10] the $4n + 2$ Hückel rule for aromaticity based on π-electron count has its counterpart in a 4-electron rule for diatropic (aromatic) circulation of induced current that is attributed to virtual translational excitations from the doubly degenerate HOMO level to the LUMO level. In the same way, the $4n$ Hückel rule for antiaromaticity of a closed-shell ground state corresponds to a 2-electron rule for paratropic (antiaromatic) circulation attributed to a rotational HOMO–LUMO excitation. These rules are *exact* only for delocalized planar annulenes in Hückel theory but, as with the Hückel rules themselves, are profitably applied to a much wider range of organic molecules.[5,9] Thus, amethyrin is, *prima facie*, expected to show 2-electron paramagnetism in the presence of a perpendicular magnetic field.

In the present work, we apply the ipsocentric method to give a direct visualisation of the induced π current density distribution in amethyrin, and of its decomposition into orbital contributions. The picture that emerges is richer than the simple 2-electron circulation expected of a notional [24]-annulene. We show that the total π current density can be partitioned into three discrete contributions that reflect the grouping of the occupied levels in the orbital energy spectrum, and their relation to the low-lying virtual levels. Two of the three are 'global', one paratropic and one diatropic, reflecting the overall symmetry of the system. The other contribution is 'local' and diatropic, reflecting the local symmetry of the six pyrrolic rings. Such a partitioning appears to be a property of the decorated macrocycles that characterize the general porphyrin family. The simple 2- and 4-electron counting rules remain largely valid, but need to be modified to account for the decoration of the macrocycle.

2. Computational details

The geometry of **1** was optimized by density functional theory (DFT) with the B3LYP functional and a 6-31G** basis set, as implemented in Gaussian98.[11] This gave an almost planar ground

[a]*School of Biosciences, University of Exeter, Exeter, UK EX4 4QD*
[b]*Department of Chemistry, University of Sheffield, Sheffield, UK S3 7HF*

state with symmetry C_2 in a very shallow energy well. There is one very small vibrational frequency, 2 cm^{-1}, and the maximum deviation from the median plane is less than 0.1 Å (0.05 Å for heavy atoms). The energy in the adjacent planar C_{2h} geometry is less than 1 kJ mol^{-1} from that of the ground state, with a one small imaginary frequency, 2*i*. It is the planar state that is used here for the discussion of the magnetic properties of the system.

The current density maps presented in this paper were computed by coupled Hartree–Fock theory using the diamagnetic-zero (DZ) variant of the continuous transformation of origin of current density (CTOCD) method[7–10] as implemented in SYSMO.[12] In this method, the current density at each point in the molecule is computed ipsocentrically, *i.e.*, by choosing the point itself as the origin of vector potential (gauge origin). Current densities induced by unit magnetic field acting at right angles to the plane of the nuclei, have been plotted in the plane at $1a_0$ above that of the nuclei. The plotting plane is close to the maximum of π current and electron density, and at this height the computed maps are insensitive to increase in basis set size beyond that of the 6-31G** set used here[13] There is also relatively little contamination from induced current density parallel to the external field,[14,15] so that the displayed current density, showing in-plane projections of current, is a good representation of the total. Contours show the modulus of current density with values 0.001×4^n a.u. (a.u. = $e/m_e a_0^4$), for $n = 0, 1, 2, \cdots$, and the arrows show the magnitude and direction of the projection of the current density vector in the plotting plane. Diatropic circulation is anticlockwise, paratropic clockwise, following the direction of circulation of the π electrons in a magnetic field pointing out of the map towards the viewer.

3. Current density maps

The π current density map for amethyrin in Fig. 1 shows the expected global paratropic (clockwise) circulation which, as in the smaller orangarin, is concentrated on the innermost pathway and dominates the global circulation. On the other hand, the map for this larger macrocycle appears to show the presence of significant local circulations within the pyrrole-like rings, suggesting a relative weakening of the dominance of the HOMO–LUMO transitions found in smaller macrocycles and simpler ring systems. An indication of current strength is given by the largest magnitude of current density, j_{max}, in the plotting plane. By this measure, with $j_{max} = 0.098$, the π current in paratropic amethyrin is just 20% stronger than in diatropic benzene ($j_{max} = 0.078$), but is weaker than in paratropic orangarin ($j_{max} = 0.115$), and substantially weaker than in diatropic sapphyrin, ($j_{max} = 0.158$).

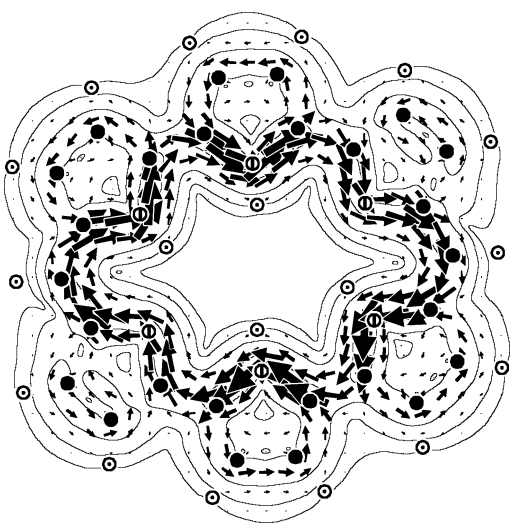

Fig. 1 Total π current density map of amethyrin. Atom symbols are: circle with dot for H, solid circle for C, bisected circle for N.

In Fig. 2 is shown part of the π orbital energy level diagram for **1**, from which the principal virtual transitions responsible for the induced current density can be identified and the corresponding pattern of ring currents deduced. In C_{2h} symmetry, selection rules for π orbital transitions in the presence of the perpendicular magnetic field are $a_u \rightarrow b_g$ for translational (electric dipole moment) transitions, and $a_u \leftrightarrow a_u$ and $b_g \leftrightarrow b_g$ for rotational (magnetic dipole moment) transitions. A strength of the ipsocentric formulation of magnetic properties is that only occupied-to-unoccupied orbital transitions need to be considered.

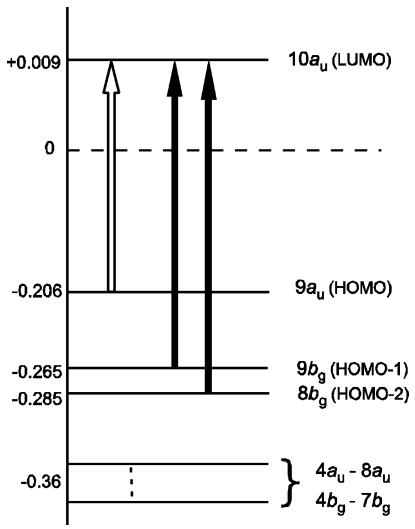

Fig. 2 Orbital energy level diagram for amethyrin showing occupied-to-unoccupied π-orbital transitions allowed by translational (black arrows) and rotational (white arrow) selection rules.

The complete π system has 36 electrons in a configuration $(a_u)^{18}(b_g)^{18}$. The $9a_u$ HOMO and $10a_u$ LUMO are partners of a split pair of orbitals with nodal symmetry corresponding to angular momentum quantum number $\lambda = 6$. The $\Delta\lambda = 0$ HOMO–LUMO transition in an annulene is rotationally allowed and is therefore expected to give rise to a paratropic global ring current. The transitions from the near-degenerate ($8b_g$, $9b_g$) pair, HOMO-1 and HOMO-2 with $\lambda = 5$, are translationally allowed and are expected to contribute to a global diatropic circulation. Such a diatropic subsystem is a standard feature that has been found to accompany the intense 2-electron paratropicity associated with a split HOMO–LUMO pair.[5,16] A group of nine lower-lying orbitals of both π symmetries between −0.36 and −0.42 E_h may give further contributions to the total current density. Lowest lying, between −0.53 and −0.61 E_h, is the "inner shell" of six orbitals belonging to the 'permutation representation' $3a_u + 3b_g$ of fully π bonding ring orbitals. These orbitals are in-phase in each contributing pyrrolic ring and, as in the monocycle itself, are not expected to

give a significant contribution to the molecular π current density. In general, the magnitude of the contribution decreases with increasing energy gap.

The distribution in shells of the 18 doubly-occupied π orbitals, together with the associated transitions to LUMO, is well simulated by the coarse-grained structure of the Hückel spectrum, and very closely by the more finely grained spectrum provided by the pseudo-π model,[17,18] showing that the essential features of the current density are properties of the topology of the system, and that the details are determined by the occupied-to-unoccupied orbital energy gaps and the corresponding transition moments.

The maps in Fig. 3 show the contributions to the current density distributions of (a) the $9a_u$ HOMO, (b) the near-degenerate ($8b_g$, $9b_g$) pair (HOMO-1, HOMO-2), (c) the sum of maps (a) and (b) for the total global current, and (d) the shell of nine lower-lying occupied orbitals, $4a_u$ to $8a_u$ and $4b_g$ to $7b_g$. We observe, in Fig. 3(a), the expected paratropic circulation of the two HOMO electrons, which, as in orangarin, follows mainly the innermost pathway, but with some bifurcation across the six pyrrolic rings. This contribution, with $j_{max} = 0.105$, is opposed by the global *diatropic* circulation, Fig. 3(b), of the four electrons in the ($8b_g$, $9b_g$) pair ($j_{max} = 0.057$) which follows the traditional 24-site conjugation pathway that would normally be considered a criterion for *paratropicity.* Note also that this contribution in amethyrin would dominate the current density in the cationic macrocycle obtained on removal of the two HOMO electrons, a process that would open a new channel for transitions to a now empty $9a_u$ orbital, and produce a global diatropic current as inferred for some heavy-atom complexes.[3] The result of the cancellation of global paratropic and diatropic circulations, shown in Fig. 3(c), is a weaker paratropic ring current ($j_{max} = 0.072$) running round the inner pathway with little bifurcation. In addition, we see also a substantial contribution, Fig. 3(d), from the shell of 18 electrons in the lower-lying orbitals clustered around energy −0.36 E_h in Fig. 2. Both translational

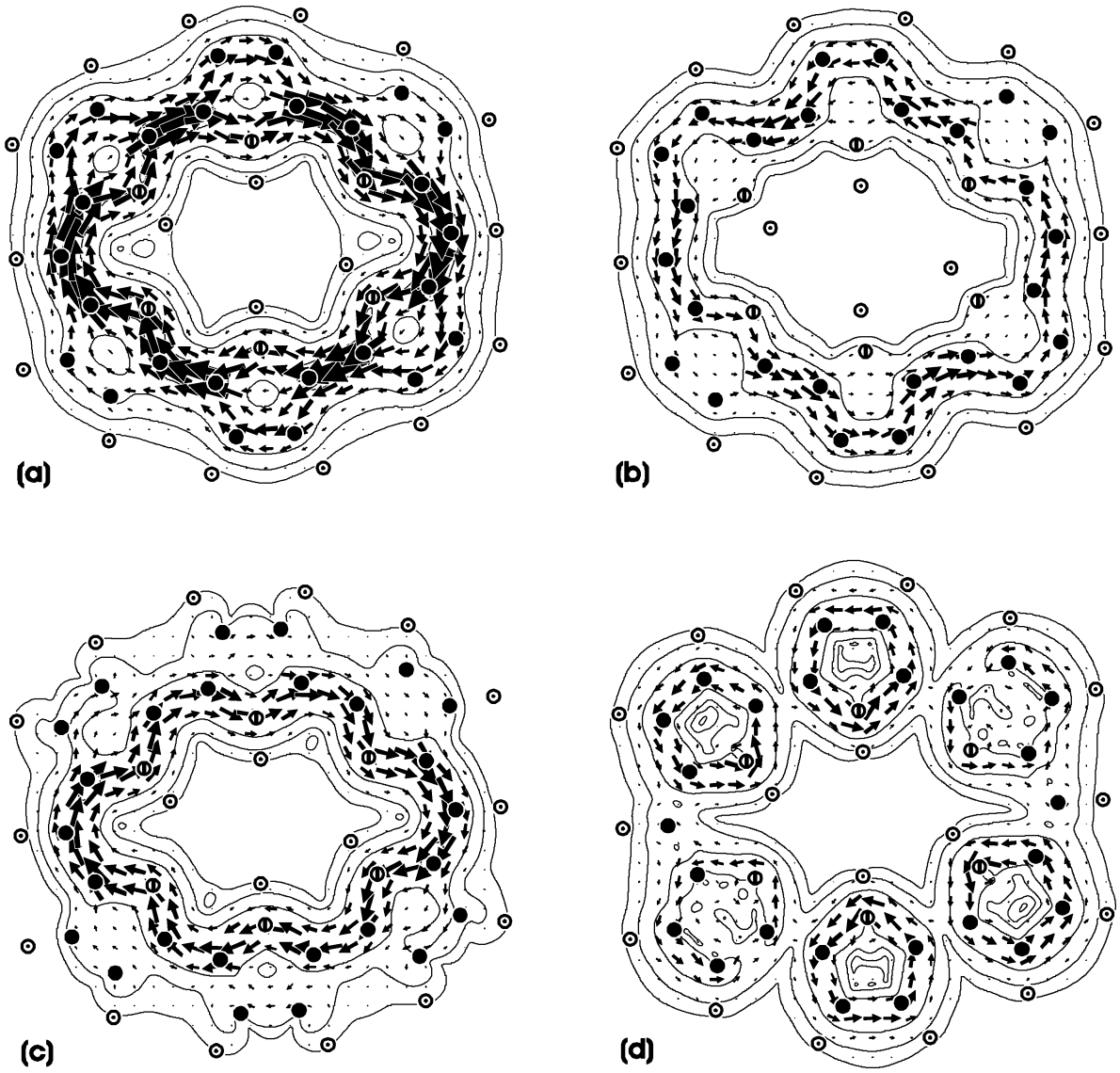

Fig. 3 Current density maps of amethyrin: (a) the global paratropic current of the $9a_u$ HOMO, (b) the global diatropic current of the ($8b_g$, $9b_g$) pair (HOMO-1, HOMO-2), (c) the sum of (a) and (b), (d) the local ring currents of the nine orbitals, $4a_u$ to $8a_u$ and $4b_g$ to $7b_g$.

and rotational transitions from this shell to virtual orbitals are allowed, and these conspire to give local ring currents in the six heterocyclic rings that decorate the main cycle. With $j_{max} = 0.056$, these local currents are only 30% weaker that in pyrrole itself (for which the same calculation gives $j_{max} = 0.081$). Finally, the lowest inner shell of 12 electrons, not represented in Figs 2 and 3, gives only nitrogen-based circulations ($j_{max} = 0.016$) in each pyrrolic subunit, which are not 'ring' currents.

4. Conclusion

In accounting for the ring current pattern in **1**, we have observed three important shells, which act as subsystems with three distinct kinds of magnetic behaviour-global paratropic, global diatropic and local diatropic. All these features arise from the molecular connectivity and are readily rationalized by inspection of orbital symmetry and nodal topology. Whilst the orbital/shell model reveals the limitations of the simplistic aromatic/antiaromatic dichotomy of the $[4n + 2]/[4n]$ annulene analogy, it also gives a framework for predictions. Reversal of the main current by oxidation/reduction of the macrocycle and tuning of the conjugation pathway and strength of current by variation of the central ion[18] are two of the consequences of the model for the more general family of (expanded) porphyrins.

References

1 J. L. Sessler, S. J. Weghorn, Y. Hiseada and V. Lynch, *Chem. Eur. J.*, 1995, **1**, 56–67.
2 J. L. Sessler and S. J. Weghorn, *Expanded, contracted and isomeric porphyrins*, Pergamon Tetrahedron Organic Chemistry Series 15, Elsevier, Amsterdam, 1997.
3 J. L. Sessler and D. Seidel, *Angew. Chem., Int. Ed.*, 2003, **43**, 5134–5175.
4 E. Steiner and P. W. Fowler, *ChemPhysChem*, 2002, **3**, 114–116.
5 E. Steiner and P. W. Fowler, *Org. Biomol. Chem.*, 2004, **2**, 34–37.
6 E. Steiner and P. W. Fowler, Mapping the Global Ring Currents in Porphyrins and Chlorins in *Chlorophylls and Bacteriochlorophylls: Biochemistry, Biophysics, Functions and Applications*, ed. B. Grimm, R. Porra, W. Rüdiger and H. Scheer, Advances in Photosynthesis and Respiration, Springer, Dordrecht, The Netherlands, 2006, vol. 25, pp. 337–347.
7 T. Keith and R. F. W. Bader, *Chem. Phys. Lett.*, 1993, **210**, 223–231.
8 P. Lazzeretti, M. Malagoli and R. Zanasi, *Chem. Phys. Lett.*, 1994, **220**, 299–304.
9 E. Steiner and P. W. Fowler, *J. Phys. Chem. A*, 2001, **105**, 9553–9562.
10 E. Steiner and P. W. Fowler, *Chem. Commun.*, 2001, 2220–2221.
11 M. J. Frisch, G. W. Trucks, H. B. Schlegel, G. E. Scuseria, M. A. Robb, J. R. Cheeseman, V. G. Zakrzewski, J. A. Montgomery, Jr., R. E. Stratmann, J. C. Burant, S. Dapprich, J. M. Millam, A. D. Daniels, K. N. Kudin, M. C. Strain, O. Farkas, J. Tomasi, V. Barone, M. Cossi, R. Cammi, B. Mennucci, C. Pomelli, C. Adamo, S. Clifford, J. Ochterski, G. A. Petersson, P. Y. Ayala, Q. Cui, K. Morokuma, D. K. Malick, A. D. Rabuck, K. Raghavachari, J. B. Foresman, J. Cioslowski, J. V. Ortiz, A. G. Baboul, B. B. Stefanov, G. Liu, A. Liashenko, P. Piskorz, I. Komaromi, R. Gomperts, R. L. Martin, D. J. Fox, T. Keith, M. A. Al-Laham, C. Y. Peng, A. Nanayakkara, C. Gonzalez, M. Challacombe, P. M. W. Gill, B. G. Johnson, W. Chen, M. W. Wong, J. L. Andres, M. Head-Gordon, E. S. Replogle and J. A. Pople, *GAUSSIAN 98 (Revision A.6)*, Gaussian, Inc., Pittsburgh, PA, 1998.
12 P. Lazzeretti and R. Zanasi, *SYSMO Package*, University of Modena, 1980; E. Steiner, P. W. Fowler, R. W. A. Havenith and A. Soncini, additional routines for evaluation and plotting of current density.
13 E. Steiner and P. W. Fowler, *Int. J. Quantum Chem.*, 1996, **60**, 609–616.
14 I. Cernušák, P. W. Fowler and E. Steiner, *Mol. Phys.*, 1997, **91**, 401–412.
15 A. Ligabue, A. Soncini and P. Lazzeretti, *J. Am. Chem. Soc.*, 2002, **124**, 2008–2014.
16 R. W. A. Havenith, L. W. Jenneskens and P. W. Fowler, *Chem. Phys. Lett.*, 2003, **367**, 468–474.
17 P. W. Fowler and E. Steiner, *Chem. Phys.Lett.*, 2002, **364**, 259–266.
18 E. Steiner, A. Soncini and P. W. Fowler, *Org. Biomol. Chem.*, 2005, **3**, 4053–4059.